

APPLICATION OF MAGNETICALLY DRIVEN TORNADO-LIKE VORTEX FOR STIRRING FLOATING PARTICLES INTO LIQUID METAL

GRANTS Ilmārs, RAEBIGER Dirk, VOGT Tobias, ECKERT Sven, GERBETH Gunter
Helmholtz-Zentrum Dresden-Rossendorf, PO Box 510119, 01314 Dresden, Germany
E-mail address of the corresponding author: i.grants@hzdr.de

Abstract: A tornado-like vortex is driven by magnetic body forces. A continuously applied rotating magnetic field provides source of the angular momentum. A pulse of a much stronger travelling magnetic field drives a converging flow that temporarily focuses this angular momentum towards the axis of the container. A highly concentrated vortex forms that produces a funnel-shaped surface depression. The ability of this vortex to entrain floating unwetted particles in liquid metal is investigated experimentally.

1 Introduction

The magnetic bar stirrer is a useful piece of standard laboratory equipment. It creates a whirlpool that somewhat resembles a tornado [1] and efficiently entrains floating powder into the liquid. The mechanics of such a flow is largely based on a simple principle. Due to angular momentum conservation the circular motion of a fluid accelerates towards the center of a converging flow. Such converging and spinning liquid metal flow may be generated by alternating magnetic fields in a fully contact-less way. A converging flow may be created by the travelling magnetic field (TMF). The angular momentum, in turn, can be injected by the rotating magnetic field (RMF). To avoid interference of both fields their frequencies should be considerably different [2]. At certain conditions when the TMF induced magnetic force is about 100 times stronger than the RMF force, this combination produces a quasi-steady concentrated vortex [2] that somewhat resembles atmospheric vortices. This vortex, however, remains blurred and does not develop a pronounced funnel on the surface. It appears not nearly as effective in entraining floating particles as the magnetic bar stirrer vortex. During the spin-up phase, however, a reproducible sharp deep vortex funnel is observed. The difference from the established flow is explained by a relatively low level of turbulence during the spin-up [3] that enables a much higher degree of vortex concentration.

Aim of the current experiment is to assess suitability of such transient flow for the purpose of stirring floating particles into the melt. If successful, such approach may be used in the technology of metal matrix composite casting.

2 Background

2.1 Magnetic forces

Let us consider a cylinder of liquid metal with constant electric conductivity σ , kinematic viscosity ν and density ρ inserted in uniform rotating and traveling magnetic fields with flux densities $B_{R,T}$ and angular frequencies $\omega_{R,T}$, respectively. The axial wave number of TMF is κ . Under the common low-frequency and low-induction conditions the RMF and

TMF induce magnetic body forces with well-known distribution [2]. The RMF induces a purely azimuthal force whose time-averaged value is given by

$$F_\phi = \sigma\omega_R B_R^2 r f(r, z), \quad (1)$$

where $f(r, z)$ is a dimensionless shape function. This force drives a rotating flow with secondary meridional circulation [4]. The dimensionless force magnitude is given by the magnetic Taylor number $Ta = \sigma\omega_R B_R^2 R_0^4 / (\rho\nu^2)$. The TMF creates an axially directed force whose time averaged value is given by [2]

$$F_z = 0.25\sigma\omega_T B_T^2 \kappa r^2. \quad (2)$$

Depending on the direction of the TMF wave vector, the liquid metal at the outer part of the container is pushed up- or downwards that drives an axi-symmetric flow torus. The dimensionless magnitude of this force is $F = \sigma\omega_T B_T^2 \kappa R_0^5 / (2\rho\nu^2)$. The magnetic flux density of both magnetic fields B_R and B_T in equation (1) and (2), respectively, is given in terms of the root mean square value. The magnetic force expressions (1,2) assume a low frequency of the respective alternating magnetic field. This is true if the shielding factor $S = \mu_0\sigma\omega_T R_0^2 < 3$, where μ_0 is the magnetic permeability [4]. This is fulfilled in our experiment.

2.2 Properties of transient tornado-like vortex

A pulse of a strong upwards directed TMF initiates a converging flow at the top surface. Because of the angular momentum conservation the azimuthal velocity attains a $\propto 1/r$ profile in the outer inviscid part of this converging flow. Being strong enough the flow produces a surface deformation on the metal surface. Depending on the RMF strength the deformation has the shape of a single sharp funnel or multiple smaller depressions rotating about a common centre (Fig. 1). This flow pattern is robust and reproducible during the initial spin-up only. As flow matures, the funnel breaks down. The initial spin-up typically lasts a few seconds [3]. There are two distinct regimes controlled by the strength of the RMF. For a weak RMF the peak swirl is much weaker than the TMF driven meridional flow and it increases with Ta while the vortex width stays invariant. For a strong RMF the peak swirl intensity stays nearly constant approaching that of the meridional flow velocity while the vortex diameter increases with Ta . The maximum swirl concentration is, thus, reached on the border between those regimes at a certain ‘‘optimum’’ RMF strength Ta_{tr} . This threshold value is a function of the TMF intensity F and it depends strongly on the type of boundary conditions at the top surface. For a free top surface $Ta_{tr}/F \propto F^{-0.625}$ while for a solid cover $Ta_{tr}/F \propto F^{-0.4}$ (Fig. 12b in [3]).

3 Experiment

3.1 Magnetic system

The inductor of combined magnetic fields KOMMA [5] has been used. At the bottom of the inductor bore there is a built-in cooling plate for directional solidification. The inductor is designed for the generation of rotating magnetic fields (RMF) and axially travelling magnetic fields (TMF) whereby the field parameters B_R, B_T, ω_R and ω_T can be controlled independently. The generation of the RMF is realized by a radial arrangement of six coils, whereby opposing coils are connected as pole-pairs. The TMF is generated

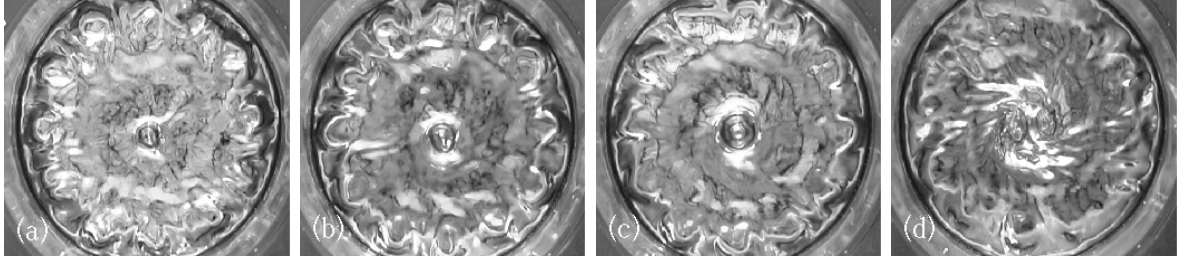


Figure 1: Snapshot of the free surface of GaInSn in a 170 mm container with a magnetically driven tornado-like vortex at $t = 1.5$ s [3]. The TMF strength is $F = 6.6 \times 10^9$; the relative RMF strength is $Ta/F = 10, 14, 25$ and 50×10^{-4} for (a–d), respectively.

inside a line-up of six coils at an equal distance of $h = 0.035$ m, yielding a wave number of $\kappa = 2\pi/6h = 30 \text{ m}^{-1}$. The frequency of the RMF is fixed to $\omega_R/2\pi = 50$ Hz and the TMF frequency is $\omega_T/2\pi = 100$ Hz in this study. Diameter of the inductor's bore is 70 mm. The TMF coils are fed by three-phase alternating current from three power amplifiers coupled to high current transformers. That allows to minimize the ramp-up time of the TMF pulse.

3.2 Particle insertion procedure

Tin is molten and overheated to 320 °C in a stainless steel mould of 50 mm diameter. Height of the molten metal is about 50 mm. Oxides and other impurities are mechanically removed from the surface. The mould is then inserted in the inductor with the RMF continuously running. After about 30 s the TMF pulse is applied and simultaneously the particles (45 μm diameter Al_2O_3 spheres) are dropped on the surface. Duration of the TMF pulse is 10 s. After the pulse the TMF induction is reduced by a factor of 1/3. The metal is then solidified under continuous RMF and TMF.

3.3 Estimates of the magnetic field strength

Formation of a sharp surface depression has been observed [3] for a value of the dimensionless parameter

$$\mathcal{F} = \frac{\sigma\omega_T B_T^2 R_0^2}{2(\rho g s)^{1/2}} \kappa R_0 = F \frac{\nu^2}{gh_c R_0^2} > 3, \quad (3)$$

where $h_c = (\gamma/\rho g)^{1/2} \approx 2.5$ mm is the capillary length, g is the gravity acceleration and γ is the surface tension. To be on the safe side, let us require $\mathcal{F} = 10$ that produces $F \approx 1.6 \times 10^8$ for tin. The magnetic field induction can now be estimated as $B_T = 75$ mT at $\omega_T/2\pi = 100$ Hz for a $2R_0 = 50$ mm mould. The following physical properties of liquid tin are assumed: $\rho = 7 \times 10^3 \text{ kg/m}^3$, $\sigma = 2 \times 10^6 \text{ S/m}$, $\nu = 10^{-6} \text{ m}^2/\text{s}$ and $\gamma = 0.5 \text{ N/m}$. Depending on the boundary conditions on the top surface, the calculated optimum RMF strength Ta_{tr} varies between 0.7×10^5 ($B_R \approx 1.4$ mT) for free-slip and 0.53×10^6 ($B_R \approx 3.9$ mT) for no-slip [3].

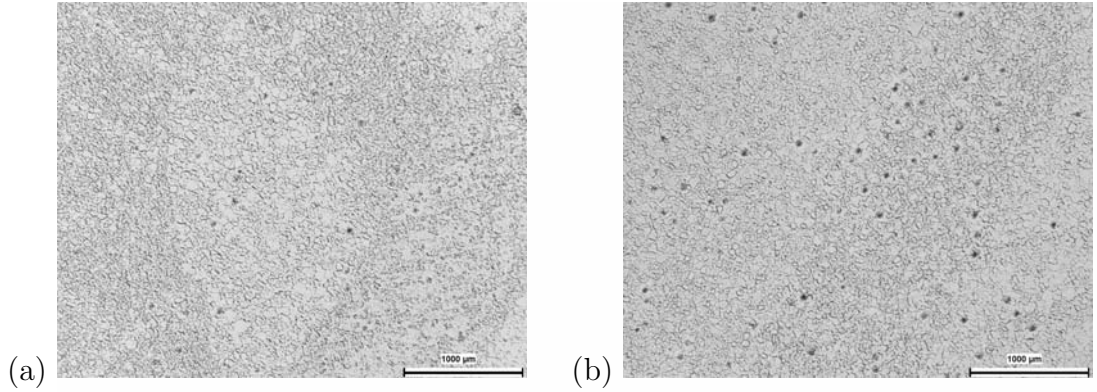


Figure 2: Microscopic views of polished tin samples with Al_2O_3 inclusions. Frame area is 12.5 mm^2 .

4 Results and discussion

The oxide layer quickly formed on the surface of the molten tin creating an uncertainty in the boundary conditions, which strongly influence the optimum RMF induction. Therefore, we first observed the surface deformation without adding particles. The oxide layer turned out to be rigid enough to resist the initial RMF driven flow. Though, the layer was broken by the spin-up vortex shortly after the beginning of the TMF pulse. The pulse only caused a significant surface deformation, when the RMF strength was at the upper limit of estimates $B_R \approx 4 \text{ mT}$ corresponding to the “optimum” for the no-slip boundary conditions. That shows that the boundary conditions influence the spin-up vortex basically through the initial conditions. In case of free-slip the upper layer of the initial flow carries considerably more angular momentum than in case of no-slip. Role of the boundary conditions appears limited to the initial state, since the shift to nearly free-slip conditions during the spin-up phase did not reduce the “optimum” RMF.

The spin-up funnel had an estimated depth of 2 to 3 cm and a duration of about two seconds. That was enough to entrain a volume of about 3 ml of particles dropped on the surface at the beginning of the pulse. This volume, however, survived the submergence and popped out of the metal immediately after the TMF pulse. This behavior may have been caused by an oxide film that enwraps the particles. Another cause could be relatively small size of the mould resulting in an insufficient level of turbulence and a too bulky funnel tip as compared to the entire flow. A better dispersion may be expected in a larger mould.

The oxide film may be prevented by an appropriate flux. The flux, however, will wet the particles and, thus, hold them trapped. This may be avoided by the following approach. In another attempt to stir the particles into the melt we alloyed them mechanically with tin into pellets. For this purpose we mixed one part of aluminum oxide particles with five parts by mass of tin powder ($45 \mu\text{m}$). The powder mixture was then mechanically pressed into 8 mm thick discs. Density of these discs was 5.2 kg/m^3 that implies porosity of about 20%. The disks were cut into pieces of a characteristic size 4 mm. The pellets (30 g) were dropped on the surface of the melt at the beginning of the TMF pulse. The spin-up vortex entrained and kept them submerged for the entire duration of the pulse. A lesser part of the pellets appeared on the surface after the pulse. The sample was solidified under a continuous TMF of $B_T = 25 \text{ mT}$ and an RMF of $B_R = 6 \text{ mT}$. Some of the submerged pellets were found at the side edge of the solidified ingot.

Apparently, they have been held attached to the mould wall by surface tension forces. Figure 2 shows two microscopic views of a section of the obtained ingot. By counting individual particles in these figures the average inter-particle distance is estimated as 0.45 mm. That corresponds to a particle volume fraction of 0.05%, at most. Thus, no more than 5% of the particles initially in the pellets were mixed into the metal. This poor performance is likely connected to the persistence of pellets even when continuously submerged. The melting time of a pellet with radius r_p is estimated as $r_p^2 \rho \Lambda / (\Delta T \lambda) \ll 10$ s, where $\Lambda = 59$ kJ/kg is the heat of fusion and $\lambda \approx 50$ W/Km the heat conductivity of tin. Thus, the metal contained in pellets should have been molten during the TMF pulse. Apparently, the pellets were held together by capillary forces forming a mixture of microscopic liquid tin droplets, aluminium oxide particles and gas voids. That would not happen if each separate particle was fully enveloped by metal. Thus, a reduced porosity and increased metal volume fraction in pellets may facilitate their disintegration.

5 Summary

Floating oxide particles are submerged into liquid metal by a spin-up vortex. Though, the particle pocket survives the high velocity flow in our experiment with a relatively small melt volume. Initial mechanical alloying with the metal facilitates particle dispersion which still remains poor in the current test. It is suggested that surface protection by flux and use of denser pellets with a lower oxide particle content may improve the efficiency of their dispersion.

Acknowledgement

Samples were kindly prepared by Mrs. M. Rossner from Division of Structural Materials at Helmholtz-Zentrum Dresden-Rossendorf. Financial support from the Helmholtz Association in form of the Alliance “Liquid Metal Technologies” is gratefully acknowledged.

References

- [1] Halász, G., Gyüre, B., Jánosi, I. M., Szabó, K.G., & Tél, T. : Vortex flow generated by a magnetic stirrer. *American J. Phys.* 75 (2007) 1092–1098.
- [2] Grants, I., Zhang, C., Eckert, S. & Gerbeth, G. : Experimental observation of swirl accumulation in a magnetically driven flow. *J. Fluid Mech.* 616 (2008) 135–152.
- [3] Vogt, T., Grants, I., Eckert, S. & Gerbeth, G. : Spin-up of a magnetically driven tornado-like vortex. *J. Fluid Mech.* (2013) 641–662.
- [4] Davidson, P. A. : Swirling flow in an axisymmetric cavity of arbitrary profile, driven by a rotating magnetic field. *J. Fluid Mech.* 254 (1992) 669–699.
- [5] Willers, B., Eckert, S., Nikrityuk P. A., Rabiger, D., Dong, J., Eckert, K., Gerbeth, G. : Efficient Melt Stirring Using Pulse Sequences of a Rotating Magnetic Field: Part II. Application to Solidification of Al-Si Alloys. *Metall. and Mat. Trans. B* 39B (2008) 304–316.